

Photogeneration of *o*-Quinone Methides from *o*-Cycloalkenylphenols

Edgar A. Leo,[†] Julio Delgado,[†] Luis R. Domingo,[‡] Amparo Espinós,[†] Miguel A. Miranda,^{*,†} and Rosa Tormos[†]

Departamento de Química-Instituto de Tecnología Química UPV-CSIC, Universidad Politécnica de Valencia, Camino de Vera s/n, 46022 Valencia, Spain, and Departamento de Química Orgánica, Instituto de Ciencia Molecular, Universidad de Valencia, Edificio Jeromi Muñoz, C/Dr. Moliner, 50, 46100 Burjassot, Valencia, Spain

mmiranda@qim.upv.es

Received June 27, 2003

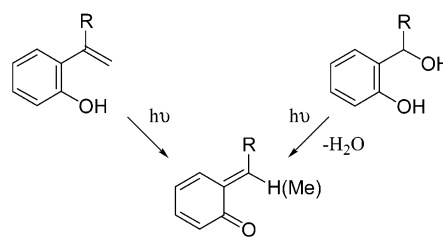
6-Alkylidenecyclohexa-2,4-dienones (*o*-quinone methides **II**) have been generated by photolysis of 2-(2'-cycloalkenyl)phenols **1** and trapped by methanol to give the ring-opened products **2**. The best results have been obtained with the cyclohexenyl derivatives **1a**, **1e**, and **1f**. In the case of the cyclopentenyl derivative **1b**, photoproduct **2b** was not observed, whereas only small amounts of **2c** and **2d** were formed from the seven- and eight-membered ring analogues **1c** and **1d**. Thus, ring size appears to be a key factor in the formation of *o*-quinone methides. This experimental result has been rationalized by means of density-functional theory (DFT) calculations. On the other hand, phenol substitution also appears to play a role in the process. Thus, electron-withdrawing groups such as CF₃ (**1f**) accelerate the reaction, whereas the opposite is true for electron-donating groups such as OCH₃ (**1e**). This is explained by an excited-state intramolecular proton transfer (ESIPT) mechanism, as the above results are consistent with the excited-state acidities of the different phenols. The lack of reactivity in the case of ketone **1g**, where the intersystem crossing quantum yield is close to unity, allows us to rule out a mechanism involving the triplet state.

Introduction

o-Quinone methides (6-alkylidenecyclohexa-2,4-dienones) are valuable synthetic intermediates with dual behavior as electrophilic and nucleophilic reagents.¹ They also have very interesting biological activity, as the actual cytotoxins responsible for the effect of some antitumor drugs, antibiotics, and DNA alkylators.²

These intermediates have been generated in several ways, including excited-state intramolecular proton transfer (ESIPT) in *o*-hydroxystyrenes or photoinduced water elimination from *o*-hydroxybenzyl alcohols (Scheme 1). They have been detected by laser flash photolysis of both precursors and exhibit characteristic transient absorption bands at 400 nm.^{3–5}

SCHEME 1. Photogeneration of *o*-Quinone Methides by ESIPT in *o*-Hydroxystyrenes (Left) or by Dehydration of *o*-Hydroxybenzyl Alcohols (Right)



In the presence of water, *o*-quinone methides undergo hydronium-ion-catalyzed hydration by a reaction mechanism involving rapid equilibrium protonation on the carbonyl oxygen followed by rate-determining nucleophilic addition of water to the ensuing carbocation. The only photoproducts are the corresponding benzyl alcohols. Other nucleophiles (MeOH, SCN⁻, Br⁻, etc.) or electron rich alkenes can also be used for trapping to give addition or cycloaddition products, respectively (Scheme 2).^{4,5}

o-Allylphenols are one-carbon homologues of *o*-hydroxystyrenes and are also known to undergo ESIPT upon irradiation; subsequent photocyclization of the resulting zwitterions leads to five- (or six-) membered ring ethers (see Scheme 3, for instance).^{6–9} Thus, insertion of a methylene group between the phenol and the

[†] Universidad Politécnica de Valencia.

[‡] Universidad de Valencia.

(1) Wan, P.; Barker, B.; Diao, L.; Fischer, M.; Shi, Y.; Yang, C. *Can. J. Chem.* **1996**, *74*, 465–475.

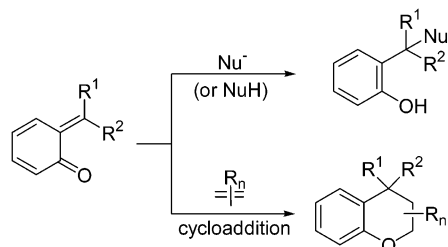
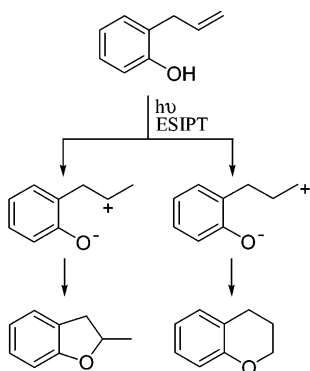
(2) (a) Peter, M. G. *Angew. Chem., Int. Ed. Engl.* **1989**, *101*, 753–757. (b) Bolton, J. L.; Pisha, E.; Zhang, F.; Qiu, S. *Chem. Res. Toxicol.* **1998**, *11*, 1113–1127. (c) Pande, P.; Shearer, J.; Yang, J.; Greenber, W. A.; Rokita, S. E. *J. Am. Chem. Soc.* **1999**, *121*, 6773–6779.

(3) (a) Foster, K. L.; Baker, S.; Brousmiche, D. W.; Wan, P. *J. Photochem. Photobiol., A* **1999**, *129*, 157–163. (b) Barker, B.; Diao, L.; Wan, P. *J. Photochem. Photobiol., A* **1997**, *104*, 91–96.

(4) (a) Chiang, Y.; Kresge, A. J.; Zhu, Y. *J. Am. Chem. Soc.* **2002**, *124*, 717–722. (b) Chiang, Y.; Kresge, A. J.; Zhu, Y. *Photochem. Photobiol. Sci.* **2002**, *1*, 67–70. (c) Chiang, Y.; Kresge, A. J.; Zhu, Y. *J. Am. Chem. Soc.* **2001**, *123*, 8089–8094. (d) Chiang, Y.; Kresge, A. J.; Zhu, Y. *J. Am. Chem. Soc.* **2000**, *122*, 9854–9855.

(5) (a) Brousmiche, D. W.; Wan, P. *J. Photochem. Photobiol., A* **2002**, *149*, 71–81. (b) Diao, L.; Yang, C.; Wan, P. *J. Am. Chem. Soc.* **1995**, *117*, 5369–5370.

(6) Fráter, G.; Schmid, H. *Helv. Chim. Acta* **1967**, *50*, 255–262.

SCHEME 2. Reaction of *o*-Quinone Methides with Nucleophiles and Dienophiles**SCHEME 3. Photocyclization of *o*-Allylphenol**

olefin moieties appears to prevent formation of *o*-quinone methides, which have never been observed in the photolysis of *o*-allylphenols.

In a preliminary communication, we have reported the generation of an *o*-quinone methide from 2-(2'-cyclohexenyl)phenol (**1a**) by initial ESIPT from the phenolic subunit to the double bond and subsequent C–C bond fragmentation, with concomitant ring opening.¹⁰ Now we report our results in full, with special emphasis on the effect of ring size and phenol substitution. Theoretical density-functional theory (DFT) calculations on the reaction pathways have also been performed to rationalize the experimental data.

Results and Discussion

Product Studies. 2-(2'-Cycloalkenyl)phenols **1a–g** (see structures in Chart 1) were prepared following the literature methods.¹¹ Compounds **1a**,⁶ **1c**,¹² and **1e**¹³ were known; their structures were confirmed by comparison of their spectroscopic data with those reported in the literature. The unknown analogues **1d**, **1f**, and **1g** were fully characterized.

(7) Horspool, W. M.; Pauson, P. L. *J. Chem. Soc., Chem. Commun.* **1967**, 22, 196–197.

(8) (a) Shani, A.; Mechoulam, R. *Tetrahedron* **1971**, 27, 601–606. (b) Chow, Y. L.; Zhou, X. M.; Gaitan, T. J.; Wu, Z. Z. *J. Am. Chem. Soc.* **1989**, 111, 3813–3818.

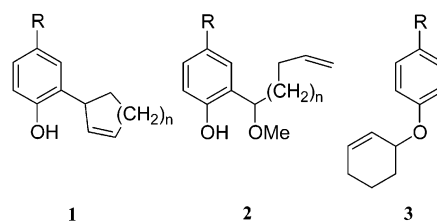
(9) (a) Miranda, M. A.; Tormos, R. *J. Org. Chem.* **1993**, 58, 3304–3307. (b) Bosch-Montalvá, M. T.; Domingo, L. R.; Jiménez, M. C.; Miranda, M. A.; Tormos, R. *J. Chem. Soc., Perkin Trans. 2* **1998**, 2175–2180.

(10) Delgado, J.; Espinós, A.; Jiménez, M. C.; Miranda, M. A. *Chem. Commun.* **2002**, 2636–2637.

(11) Tarbell, D. S. The Claisen rearrangement. In *Organic Reactions*; Adams, R., Ed.; Wiley: New York, 1944; Vol. 2, pp 1–48.

(12) Cristol, S. J.; Ilenda, C. S. *J. Am. Chem. Soc.* **1975**, 97, 5862–5867.

(13) Hosokawa, T.; Miyagi, S.; Murahashi, S.; Sonoda, A.; Matsuura, Y.; Tanimoto, S.; Kakudo, M. *J. Org. Chem.* **1978**, 43, 719–724.

CHART 1

	R	n
a	H	2
b	H	1
c	H	3
d	H	4
e	OCH ₃	2
f	CF ₃	2
g	COCH ₃	2

The absorption spectra of **1a–g** showed their most intense band below 300 nm, so the irradiation experiments were performed using quartz-filtered light. All samples (in methanolic solution) were deoxygenated with argon before irradiation. The photomixtures were analyzed by GC, GC–MS, and ¹H NMR. Then, they were submitted to column chromatography to isolate the pure photoproducts.

Ring-opened methanol adducts (**2**) were obtained in all cases except for **1b** and **1g**. These photoproducts present characteristic signals in ¹H NMR, mainly due to the terminal olefinic protons, the methoxy group, and a very deshielded H-bonded hydroxylic proton. The mass spectral fragmentation was also very characteristic; the base peak always corresponded to the benzylic fragmentation. All carbon atoms gave distinct signals in ¹³C NMR in the expected δ ranges.

Effect of the Cycloalkenyl Ring Size. Although the methanol adducts **2** were the only well-defined photoproducts, cycloalkenyl ring size was a critical factor as regards the reaction efficiency. The best results for the unsubstituted phenols were obtained with the six-membered ring compound **1a** (ca. 55% yield after 6 h; in addition, 10% of the unreacted starting material was recovered and ca. 35% of an unidentified polymer was formed). In the case of the cyclopentenyl derivative **1b**, not even traces of any product assignable to **2b** were detected by GC–MS or ¹H NMR. With the seven- and eight-membered ring analogues **1c** and **1d**, only small amounts of the corresponding photoproducts **2c** and **2d** (ca. 5%) were obtained under the same reaction conditions. Prolonged irradiation of **1b–d** resulted in the formation of significant amounts of polymer.

Effect of Phenol Substitution. Three para-substituted phenols were selected with different electron donor or withdrawing groups. Compound **1g**, with an acetyl substituent, was photostable so that no photoproduct was observed. The relative photoreaction rates for **1e** and **1f** are shown in Figure 1, using the unsubstituted compound **1a** for comparison. From these data, it is clear that electron-withdrawing substituents (such as CF₃) accelerate the process, whereas electron-donating groups (such as OMe) have the opposite effect. Nonetheless, the reaction was clean in the three cases, and moderate to good yields of the photoproducts were obtained (up to 43%

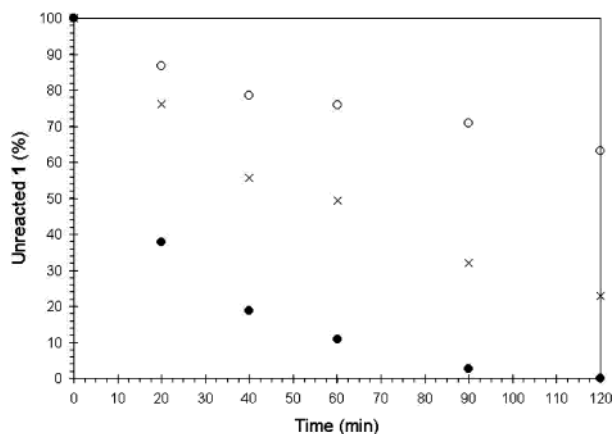
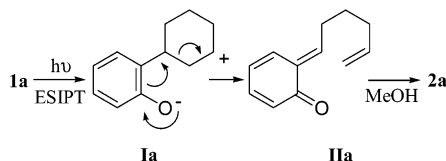


FIGURE 1. Kinetics of the photoreaction for **1a** (×), **1e** (○), and **1f** (●).

SCHEME 4. Mechanism Which Explains the Formation of 2a by Irradiation of 1a in Methanol



of **2e** and 88% of **2f**) when the irradiations were conveniently prolonged.

Reaction Mechanism. The proposed reaction mechanism to explain the formation of **2a** is outlined in Scheme 4. This mechanism could be extended to all of the *o*-cycloalkenylphenols studied.

Initial ESIPT would occur from the phenol subunit to the cycloalkenyl double bond, generating the zwitterionic intermediate **Ia**. Subsequently, **Ia** would undergo C–C bond fragmentation with concomitant ring opening, leading to *o*-quinone methide **IIa**. Because irradiations were performed using methanol as the solvent, intermediate **IIa** would be readily trapped to give the final product **2a**.

The involved excited state must be of singlet nature, because compound **1g** (where the intersystem-crossing quantum yield must be near unity, as expected for a substituted acetophenone)¹⁴ is unreactive.

Excited-State Acidity. To understand the effect of the phenol substituent on the reaction rates, the acidity of the lowest lying singlet excited state (pK_a^*) was determined for phenols **1a**, **1e**, and **1f**, as this property must be directly related to the feasibility of the key ESIPT step. This was achieved by using the Förster cycle, which is based on the known acidities in the ground state (pK_a) and on the singlet energies of the phenols and their conjugated bases (phenolates), obtained from the insertion point of both normalized absorption and fluorescence spectra in neutral and basic methanolic media.^{15–18} The results are shown in Table 1.

TABLE 1. Excited-Singlet-State Acidities (pK_a^*) for Phenols 1a, 1e, and 1f in Methanol, Calculated Using the Förster Cycle

	E_{HA}^a	$E_{A^-}^a$	pK_a^b	pK_a^*
1a	100.7	93.0	10.00	4.52
1e	93.3	86.6	10.21	5.29
1f	101.2	93.1	8.68	2.71

^a Singlet energies of the phenols (E_{HA}) and their conjugated bases (E_{A^-}) in kcal/mol. ^b pK_a values were taken from the literature.^{15,18} They were assumed to be approximately the same in water and in methanol, which was also used for the absorption–fluorescence measurements.

TABLE 2. Total (in au) and Relative^a (in kcal/mol, in Parentheses) Energies of the Reactants, Intermediates, and Transition States (TS) Involved in the Isomerization of 1a and 1b into IIa and IIb

	(S_0) ^b	(S_1) ^c	
1a	–540.915 165	–540.735 429	(112.8)
1a		–540.772 471	(89.5)
TSa	–540.834 771	–540.754 279	(101.0)
IIa	–540.874 457	–540.774 704	(88.1)
1b	–501.597 181	–501.415 133	(114.2)
1b		–501.465 569	(82.6)
TSb	–501.516 561	–501.435 332	(101.6)
IIb	–501.560 293	–501.459 647	(86.3)

^a Relative to **1a** (S_0) and **1b** (S_0). ^b B3LYP/6-31G* calculations. ^c CIS (singlet) calculations.

Qualitatively, the obtained pK_a^* values are consistent with the relative photoreaction rates. Thus, **1f** was the most reactive of the three phenols, followed by **1a** and then by **1e**; the same order was found for the excited-state acidities. Hence, the relative reactivities of the three substrates support the proposed ESIPT mechanism.

Theoretical Calculations. The reaction mechanism for the photoisomerization of 2-(2'-cyclohexenylphenol) **1a** to the *o*-quinone methide **IIa** was theoretically studied using density-functional theory (DFT) methods (see Computational Methods in the Experimental Section). After exhaustive exploration of the potential energy surface (PES) for the isomerization process at the ground state (S_0), a transition structure (TS) connecting both isomers was found and characterized: **TSa**. The total and relative energies of the stationary points located at the S_0 state, together with the computed S_1 energies, are presented in Table 2, and the geometries of the different species **1a**, **Ia**, **IIa**, and **TSa** are given in Figure 2.

Thermal isomerization of 2-(2'-cyclohexenyl)phenol **1a** (S_0) to the *o*-quinone methide **IIa** (S_0) presents a barrier of 50.4 kcal/mol. This very large value clearly prevents the isomerization process. In addition, the reaction is very endothermic, 25.5 kcal/mol. Therefore, under thermal equilibration conditions, formation of *o*-quinone methide **IIa** is kinetically and thermodynamically very unfavorable.

The calculated energy for the configuration interactions including only single electronic vertical excitation (CIS) of **1a** (S_0) to **1a** (S_1) is 112.8 kcal/mol. This species could be converted into the more stable **Ia** (S_1), which lies 23.3 kcal/mol below **1a** (S_1). The CIS barrier for the transformation of **Ia** (S_1) into **IIa** (S_1), via **TSa** (S_1), is 11.5 kcal/

(14) Murov, S. L.; Carmichael, I.; Hug, G. L. *Handbook of Photochemistry*, 2nd ed.; Marcel Dekker: New York, 1993; p 4.

(15) Wehry, E. L.; Rogers, L. B. *J. Am. Chem. Soc.* **1965**, *87*, 4234–4238.

(16) Marciniak, B.; Kozubek, H.; Paszyc, S. *J. Chem. Educ.* **1992**, *69*, 247–249.

(17) Förster, T. *Z. Elektrochem.* **1950**, *54*, 521–535.

(18) Liotta, C. L.; Smith, D. F.; Hopkins, H. P.; Rhodes, K. A. *J. Phys. Chem.* **1972**, *76*, 1909–1912.

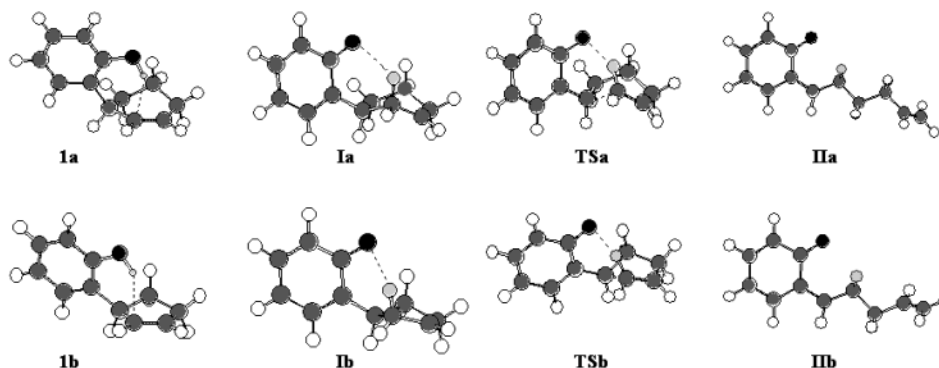


FIGURE 2. Structures of the stationary points involved in the photoisomerization of **1a** and **1b** into **IIa** and **IIb**. Compounds **1a** and **1b** present an intramolecular OH–C interaction between the phenol hydrogen atom and the π system of the C2–C3 double bond, indicated with dotted lines.

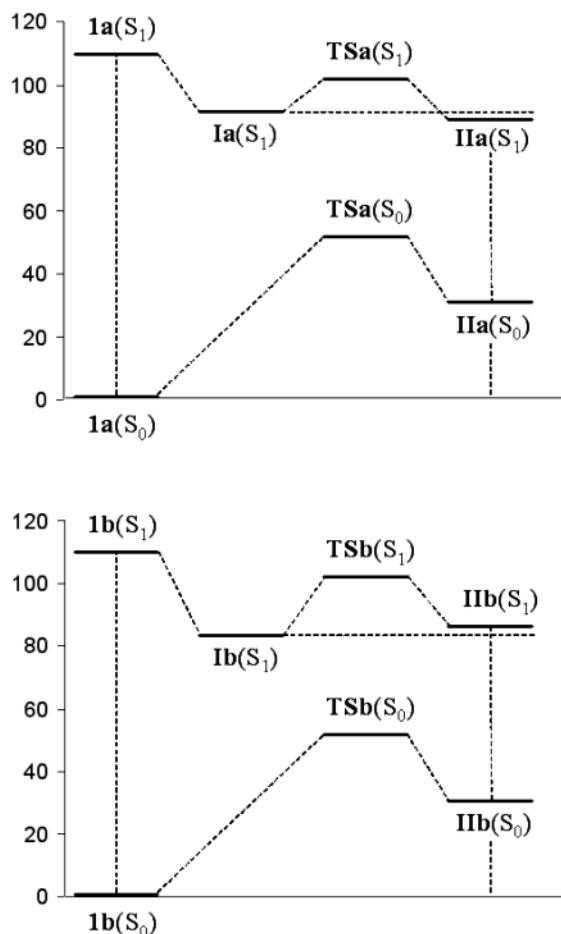


FIGURE 3. Energy profile (in kcal/mol) for the isomerization of **1a** into **IIa** and **1b** into **IIb**, at the S_0 and S_1 states.

mol. In addition, transformation of **Ia** (S_1) into **IIa** (S_1) is slightly exothermic by 1.4 kcal/mol. These values allow us to understand the conversion of intermediate **Ia** (S_1) into **IIa** (S_1). Finally, deexcitation of **IIa** (S_1) allows formation of **IIa** (S_0). A schematic representation of the PES for the transformation of **1a** into **IIa** at the S_0 and S_1 states is given in Figure 3.

To investigate the effects of ring size on the photoisomerization process, the S_1 energies for the experimentally unfavorable transformation of 2-cyclopentenylphenol **1b** into its corresponding *o*-quinone methide **IIb** were

also computed. This reaction was chosen because it was the least efficient in the series. Again, the relative energies are given in Table 2, and the corresponding geometries are shown in Figure 2. In the ground state, the isomerization process for 2-(2'-cyclopentenyl)phenol **1b** is slightly less endothermic, 23.1 kcal/mol, than for the 2-(2'-cyclohexenyl)phenol **1a**. It presents a similar barrier (50.6 kcal/mol), but it is still unfavorable. In the excited state, the barrier for the ring-opening process at intermediate **Ib** (S_1) is 19.0 kcal/mol, significantly higher than the value found for **Ia**. In addition, transformation of **Ib** (S_1) into **IIb** (S_1) is endothermic by 3.7 kcal/mol. These results could explain the lack of isomerization of **1b** into **IIb**. The larger barrier found for the bond-breaking process at the intermediate **Ib** compared to **Ia** is attributable to the larger stabilization of the former (see Table 2). This stabilization is associated with the relief of strain when hybridization changes from sp^2 to sp^3 at the C2 carbon atom belonging to the cyclopentene ring present in **1b** (S_1).

Conclusion

In summary, we have gained further mechanistic insight into the formation of 6-alkylidenecyclohexa-2,4-dienones (*o*-quinone methides) by photolysis of *o*-cycloalkenylphenols. Ring size appears to be a critical factor in the process; the best results are obtained with the cyclohexenyl derivatives. This is rationalized by DFT calculations. The reaction efficiency also depends on phenol substitution: electron-withdrawing groups accelerate the reaction, whereas the reverse is true for electron-donating substituents. This is consistent with an ESIPT mechanism, as evidenced by the relative acidity of the different phenols in their singlet excited states. Finally, the reaction does not take place for the excited triplet states, as shown by the lack of reaction in the case of ketone **1g**.

Experimental Section

2-(2'-Cyclooctenyl)phenol (1d). Oil. FTIR ν_{\max} (cm^{-1}): 3610 (OH), 3498 (OH). ^1H NMR (CDCl_3 , 300 MHz, δ): 7.22–6.82 (m, 4H), 5.90 (m, 1H), 5.49 (t, 1H, $J = 10$ Hz), 5.33 (s, 1H), 4.00–3.86 (m, 1H), 2.55–2.15 (m, 2H), 2.00–1.20 (m, 8H). ^{13}C NMR (CDCl_3 , 75 MHz, δ): 154.2 (C), 132.9 (CH), 132.3 (CH), 131.8 (C), 127.3 (CH), 126.6 (CH), 120.8 (CH), 115.9 (CH), 35.3 (CH), 33.9 (CH_2), 29.7 (CH_2), 26.7 (CH_2), 26.6 (CH_2).

25.6 (CH₂). MS *m/z* (%): 202 (M⁺, 75), 159 (34), 145 (46), 131 (32), 120 (84), 107 (100), 95 (37), 91 (23), 77 (23). HRMS *m/z*: calcd for C₁₄H₁₈O, 202.1358; found, 202.1364.

2-(2'-Cyclohexenyl)-4-trifluoromethylphenol (1f). Oil. FTIR ν_{\max} (cm⁻¹): 3602 (OH), 3471 (OH). ¹H NMR (CDCl₃, 300 MHz, δ): 7.37 (m, 2H), 6.86 (d, 1H, *J* = 9 Hz), 6.10 (m, 1H), 5.75 (m, 2H), 3.61 (m, 1H), 2.30–1.40 (m, 6H). ¹³C NMR (CDCl₃, 300 MHz, δ): 156.8 (C), 131.9 (CH), 131.8 (C), 128.6 (CH), 126.8 (CH), 124.9 (C), 124.8 (CH), 120.1 (C), 116.2 (CH), 37.9 (CH), 29.7 (CH₂), 24.9 (CH₂), 21.2 (CH₂). MS *m/z* (%): 242 (M⁺, 100), 227 (45), 223 (17), 213 (38), 199 (51), 188 (35), 175 (15), 145 (29). HRMS *m/z*: calcd for C₁₃H₁₃OF₃, 242.0919; found, 242.0917.

2-(2'-Cyclohexenyl)-4-acetylphenol (1g). Solid, mp 99–100 °C. Recrystallized from CH₂Cl₂/hexane. FTIR ν_{\max} (cm⁻¹): 3600 (OH), 3458 (OH), 1680 (C=O). ¹H NMR (CDCl₃, 300 MHz, δ): 7.8–7.74 (m, 2H), 6.85 (d, 1H, *J* = 8 Hz), 6.15–6.06 (m, 2H), 5.86–5.80 (m, 1H), 3.61 (m, 1H), 2.55 (s, 3H), 2.20–1.50 (m, 6H). ¹³C NMR (CDCl₃, 75 MHz, δ): 199.1 (C), 159.9 (C), 132.5 (CH), 131.0 (CH), 130.7 (C), 130.0 (C), 129.6 (CH), 129.4 (CH), 116.1 (CH), 36.8 (CH), 30.3 (CH₂), 26.8 (CH₃), 25.4 (CH₂), 21.6 (CH₂). MS *m/z* (%): 216 (M⁺, 70), 201 (100), 173 (15), 145 (16). HRMS *m/z*: calcd for C₁₄H₁₆O₂, 216.1150; found, 216.1150. Anal. Calcd for C₁₄H₁₆O₂: C, 77.81; H, 7.46. Found: C, 77.36; H, 7.35.

2-(1-Methoxy-5-hexenyl)phenol (2a). Oil. FTIR ν_{\max} (cm⁻¹): 3378 (OH), 1244. ¹H NMR (CDCl₃, 300 MHz, δ): 7.94 (s, 1H), 7.24–7.14 (m, 1H), 6.96–6.78 (m, 3H), 5.84–5.68 (m, 1H), 5.04 (m, 2H), 4.25 (t, 1H, *J* = 7 Hz), 3.39 (s, 3H), 2.10–1.30 (m, 6H). ¹³C NMR (CDCl₃, 75 MHz, δ): 155.3 (C), 138.4 (CH), 129.0 (CH), 128.4 (CH), 124.9 (C), 119.6 (CH), 116.8 (CH), 114.8 (CH₂), 86.0 (CH), 57.3 (CH₃), 35.4 (CH₂), 33.1 (CH₂), 25.1 (CH₂). MS *m/z* (%): 206 (M⁺, 25), 174 (57), 159 (17), 146 (20), 137 (100), 133 (60), 131 (25), 120 (25), 107 (16). HRMS *m/z*: calcd for C₁₃H₁₈O₂, 206.1307; found, 206.1354.

2-(1-Methoxy-7-octenyl)phenol (2d). Oil. FTIR ν_{\max} (cm⁻¹): 3377 (OH), 1243. ¹H NMR (CDCl₃, 300 MHz, δ): 7.92 (s, 1H), 7.20–7.12 (m, 1H), 6.94–6.76 (m, 3H), 5.84–5.68 (m, 1H), 5.00–4.86 (m, 2H), 4.21 (t, 1H, *J* = 7 Hz), 3.36 (s, 3H), 2.06–1.16 (m, 10H). ¹³C NMR (CDCl₃, 75 MHz, δ): 138.4 (CH), 128.9 (CH), 128.4 (CH), 124.5 (C), 119.6 (CH), 116.8 (CH), 114.3 (CH₂), 86.1 (CH), 57.2 (CH₃), 35.9 (CH₂), 33.6 (CH₂), 28.8 (CH₂), 28.7 (CH₂), 25.6 (CH₂). MS *m/z* (%): 234 (M⁺, 18), 202 (10), 137 (100), 133 (29), 120 (41), 107 (43). HRMS *m/z*: calcd for C₁₅H₂₂O₂, 234.1620; found, 234.1630.

4-Methoxy-2-(1-methoxy-5-hexenyl)phenol (2e). Oil. FTIR ν_{\max} (cm⁻¹): 3400 (OH), 1270, 1240. ¹H NMR (CDCl₃, 300 MHz, δ): 7.50 (s, 1H), 6.82–6.71 (m, 2H), 6.50 (d, 1H, *J* = 3 Hz), 5.82–5.66 (m, 1H), 5.20–4.86 (m, 2H), 4.16 (t, 1H, *J* = 7 Hz), 3.73 (s, 3H), 3.36 (s, 3H), 2.2–1.4 (m, 6H). ¹³C NMR (CDCl₃, 75 MHz, δ): 153.3 (C), 149.7 (C), 138.7 (CH), 126.0 (C), 117.7 (CH), 115.2 (CH), 114.5 and 114.1 (CH and CH₂), 86.2 (CH), 57.7 (CH₃), 56.1 (CH₃), 35.7 (CH₂), 33.9 (CH₂), 25.5 (CH₂). MS *m/z* (%): 236 (M⁺, 22), 204 (100), 189 (12), 175 (10), 163 (74), 161 (22), 152 (18), 150 (30), 137 (24), 107 (10). HRMS *m/z*: calcd for C₁₄H₂₀O₃, 236.1412; found, 236.1431.

2-(1-Methoxy-5-hexenyl)-4-trifluoromethylphenol (2f). Oil. FTIR ν_{\max} (cm⁻¹): 3346 (OH), 1329, 1126. ¹H NMR (CDCl₃, 300 MHz, δ): 8.39 (s, 1H), 7.45 (dd, 1H, *J*₁ = 8 Hz, *J*₂ = 2 Hz), 7.20 (m, 1H), 6.93 (d, 1H, *J* = 8 Hz), 5.86–5.68 (m, 1H), 5.06–4.90 (m, 2H), 4.30 (dd, 1H, *J*₁ = 8 Hz, *J*₂ = 6 Hz), 2.03–1.30 (m, 6H). ¹³C NMR (CDCl₃, 75 MHz, δ): 158.3 (C), 138.1 (CH), 126.3 (CH), 125.5 (CH), 121.8 (C), 117.2 (CH), 115.0 (CH₂), 85.6 (CH), 57.6 (CH₃), 35.3 (CH₂), 33.4 (CH₂), 24.9 (CH₂). MS *m/z* (%): 274 (M⁺, 6), 242 (20), 227 (11), 205 (100), 201 (27), 188 (17), 175 (14). HRMS *m/z*: calcd for C₁₄H₁₇O₂F₃, 274.1181; found, 274.1174.

1-(2'-Cyclohexenyl)-4-trifluoromethylbenzene (3f). Oil. FTIR ν_{\max} (cm⁻¹): 1165. ¹H NMR (CDCl₃, 300 MHz, δ): 7.53 (d, 2H, *J* = 8 Hz), 6.97 (d, 2H, *J* = 8 Hz), 6.06–5.98 (m, 1H), 5.90–5.80 (m, 1H), 4.85 (m, 1H), 2.26–1.56 (m, 6H). ¹³C

NMR (CDCl₃, 75 MHz, δ): 160.0 (C), 132.8 (CH), 126.9 (CH), 125.4 (CH), 122.3 (C), 115.5 (CH), 71.0 (CH), 28.1 (CH₂), 25.0 (CH₂), 18.8 (CH₂). MS *m/z* (%): 242 (M⁺, 3), 162 (4), 143 (9), 81 (100), 80 (48), 79 (27). HRMS *m/z*: calcd for C₁₃H₁₃OF₃, 242.0919; found, 242.0943.

4-(2'-Cyclohexenyl)acetophenone (3g). Solid, mp 47–49 °C. Recrystallized from CH₂Cl₂/hexane. FTIR ν_{\max} (cm⁻¹): 1684 (C=O), 1170. ¹H NMR (CDCl₃, 300 MHz, δ): 7.92 (d, 2H, *J* = 9 Hz), 6.94 (d, 2H, *J* = 9 Hz), 6.05–5.96 (m, 1H), 5.88–5.81 (m, 1H), 4.89 (m, 1H), 2.55 (s, 3H), 2.45–1.50 (m, 6H). ¹³C NMR (CDCl₃, 75 MHz, δ): 196.6 (C), 161.8 (C), 132.8 (CH), 130.5 (CH), 129.9 (C), 125.3 (CH), 115.0 (CH), 70.8 (CH), 28.0 (CH₂), 26.2 (CH₃), 24.9 (CH₂), 18.7 (CH₂). MS *m/z* (%): 216 (M⁺, 7), 137 (100), 121 (26), 81 (85), 79 (56), 78 (26). HRMS *m/z*: calcd for C₁₄H₁₆O₂, 216.1150; found, 216.1142. Anal. Calcd for C₁₄H₁₆O₂: C, 77.81; H, 7.46. Found: C, 77.67; H, 7.55.

Computational Methods. To evaluate the energies of the intermediates and transition states in the excited singlet (S₁) state, the PES at the triplet (T₁) excited state was first studied. Then, the optimized triplet geometries were assumed to be the same as in S₁, and hence, they were used to obtain the S₁ energies.

Density-functional theory¹⁹ calculations have been carried out using the B3LYP or UB3LYP²⁰ methods, together with the standard 6-31G* basis set.²¹ The geometry optimizations of singlet (S₀) or triplet (T₁) states were carried out using the Bery analytical gradient optimization method.²² For minimized triplet states, the UB3LYP wave functions showed nonspin contamination ($\langle s^2 \rangle \approx 2.0$). Energies for the excited singlet (S₁) states were evaluated by configuration interaction calculations including only single electronic excitations (CIS).²³ All calculations were carried out with the Gaussian 98 suite of programs.²⁴

Acknowledgment. Financial support from the Spanish MCYT (Grants BQU2001-2725 and BQU2002-01032), the Generalitat Valenciana (Grant GV01-272), and the Fundación José y Ana Royo (fellowship to E.A.L.) is gratefully acknowledged.

Supporting Information Available: General experimental procedures and ¹H and ¹³C NMR spectra of compounds **1d**, **1f**, **1g**, **2a**, **2d**, **2e**, **2f**, **3f**, and **3g**. This material is available free of charge via the Internet at <http://pubs.acs.org>.

JO034918V

(19) (a) Parr, R. G.; Yang, W. *Density Functional Theory of Atoms and Molecules*; Oxford University Press: New York, 1989. (b) Ziegler, T. *Chem. Rev.* **1991**, *91*, 651–667.

(20) (a) Becke, A. D. *J. Chem. Phys.* **1993**, *98*, 5648–5652. (b) Lee, C.; Yang, W.; Parr, R. G. *Phys. Rev. B* **1988**, *37*, 785–789.

(21) Hefre, W. J.; Radom, L.; Schleyer, P. v. R.; Pople, J. A. *Ab Initio Molecular Orbital Theory*; Wiley: New York, 1986.

(22) (a) Schlegel, H. B. *J. Comput. Chem.* **1982**, *3*, 214–218. (b) Schlegel, H. B. *Geometry Optimization on Potential Energy Surfaces*. In *Modern Electronic Structure Theory*; Yarkony, D. R., Ed.; World Scientific Publishing: Singapore, 1994.

(23) Foresman, J. B.; Head-Gordon, M.; Pople, J. A.; Frisch, M. J. *J. Phys. Chem.* **1992**, *96*, 135–149.

(24) Frisch, M. J.; Trucks, G. W.; Schlegel, H. B.; Scuseria, G. E.; Robb, M. A.; Cheeseman, J. R.; Zakrzewski, V. G.; Montgomery, J. A., Jr.; Stratmann, R. E.; Burant, J. C.; Dapprich, S.; Millam, J. M.; Daniels, A. D.; Kudin, K. N.; Strain, M. C.; Farkas, O.; Tomasi, J.; Barone, V.; Cossi, M.; Cammi, R.; Mennucci, B.; Pomelli, C.; Adamo, C.; Clifford, S.; Ochterski, J.; Petersson, G. A.; Ayala, P. Y.; Cui, Q.; Morokuma, K.; Malick, D. K.; Rabuck, A. D.; Raghavachari, K.; Foresman, J. B.; Cioslowski, J.; Ortiz, J. V.; Stefanov, B. B.; Liu, G.; Liashenko, A.; Piskorz, P.; Komaromi, I.; Gomperts, R.; Martin, R. L.; Fox, D. J.; Keith, T.; Al-Laham, M. A.; Peng, C. Y.; Nonayakkara, A.; Gonzalez, C.; Challacombe, M.; Gill, P. M. W.; Johnson, B. G.; Chen, W.; Wong, M. W.; Andres, J. L.; Head-Gordon, M.; Replogle, E. S.; Pople, J. A. *Gaussian 98*, revision A.6; Gaussian, Inc.: Pittsburgh, PA, 1998.